ECE

WEMPEC

Wisconsin Electric Machines and Power Electronics Consortium

RESEARCH REPORT
84-11

Hybrid Computer Simulation of a Field Oriented Induction Motor Drive

T. Matsuo
Mitsubishi Electric Co.
Kobe, Japan

T.A. Lipo
University of Wisconsin
Madison, Wisconsin

Department of Electrical and Computer Engineering
University of Wisconsin-Madison
Madison, Wisconsin 53706

October 1984

HYBRID COMPUTER SIMULATION OF A FIELD ORIENTED INDUCTION MOTOR DRIVE

T. Matsuo
Mitsubishi Electric Corp.
Kobe, Japan

T.A. Lipo
University of Wisconsin
Madison, Wisconsin

Abstract

The principle of field oriented control of adjustable speed induction motor drives rapidly becoming the accepted control method for high response applications. This paper describes briefly the motor control principles involved in field oriented control and outlines how such a control is mechanized in hardware. A detailed simulation of an indirect type of field oriented control is described. In particular, attention is given to the implementation of a hysteresis type of PWM current regulated type of inverter. A number of computer simulation traces are shown which demonstrate the desirable control features of field orientation.

Introduction

Field oriented techniques incorporating microprocessors have made possible the application of induction motor drives in high performance applications where only DC motor drives were previously available. Probably the most widely used scheme, shown in Fig. 1 and devised by Hasse [1], is an indirect flux sensing method wherein the rotor flux is estimated from the stator current vector, voltage vector and/or rotor speed. This estimate is, in effect, fed forward to the flux and torque controller. Because of the use of the concept of viewing the machine voltages, currents and flux as vectors, such control systems are frequently referred to as *vector controllers*.

Vector control principles can be applied without regard to the type of inverter and VVI (variable voltage source six step), CSI (current source) inverters as well as cycloconverters have been used as the frequency converter. However, the recent activity in the development of high power bipolar transistors as well as other power switches which have led to high power devices with inherent turn off as well as turn on capabilities and has made the so called *current regulated PWM inverter* the widespread choice in fast response AC servo applications [2- 4]. This approach employs a fast switching PWM inverter to control the current supplied to the motor on an almost instantaneous basis. The inverter appears as nearly an ideal current source to the motor provided that the switching of the inverter power devices is sufficiently fast relative to the frequency desired. The substantial development cost of such a drive together with the close similarity of an analog computer simulation to an actual implemention of the control in hardware makes a computer simulation of such a drive an important design tool. This paper describes analog and hybrid computer simulation techniques for the indirect field oriented control technique as applied to a such a current regulated PWM inverter drive.

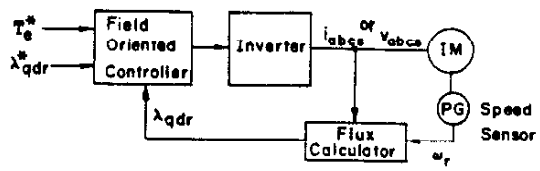

Fig. 1 Equivalent Circuit of an Indirect Field Oriented Induction Motor Controller.

Induction Machine Representation for Vector Control

The dynamic behavior of a three phase, three wire induction motor with a squirrel-cage rotor or a short circuited wound rotor can be conveniently described by vector equations in a d-q rotating reference frame [5]. With the appropriate constraints, the d-q frame can be made to rotate synchronously with the stator or rotor voltage, current or flux vectors. The so-called field coordinate systems are obtained when the d-q frame rotates synchronously with the magnetic field (magnetic flux) within the machine. It is useful for purposes of motor control to allow the reference frame to rotate synchronously with the rotor flux vector (rotor field coordinates). If the angular velocity ω_e is used to represent the instantaneous angular speed of the rotor flux vector, then the equations which describe the transient behavior of an induction motor can be written as [5]

$$\mathbf{v}_{qds}^e = \left[r_s + L_s \left(\frac{d}{dt} + \omega_e \times \right) \right] \mathbf{i}_{qds}^e + L_m \left(\frac{d}{dt} + \omega_e \times \right) \mathbf{i}_{qdr}^e \qquad (1)$$

and

$$0 = L_m \left[\frac{d}{dt} + (\omega_e - \omega_r) \times \right] \mathbf{i}^e_{qds} + \left\{ r_r' + L_r' \left[\frac{d}{dt} + (\omega_e - \omega_r) \times \right] \right\} \mathbf{i}^e_{qdr} \quad (2)$$

$$T_e = \frac{3}{2} \frac{P}{2} L_m \, \mathbf{i}^e_{qdr} \times \mathbf{i}^e_{qds} \quad (3)$$

$$T_e - T_L = \frac{2}{P} J \frac{d\omega_r}{dt} \quad (4)$$

In these equations the bold faced quantities are three dimensional cartesian vectors which, without a zero sequence component, can be considered as rotating on the d-q plane [5]. With no zero sequence, the stator d-q voltage vector is given as

$$\mathbf{v}^e_{qds} = \left[v^e_{qs}, v^e_{ds}, 0 \right]^t \quad (5)$$

The superscript t in Eq. 5 denotes the vector transpose and the superscript e signifies that the vector is represented in a synchronously rotating reference frame, which is, in this case, rotating synchronously with the rotor flux vector. Note that in Eq. 5 provision is made for a third, zero sequence, component, v^e_{ns}. However, this term has been set to zero since only a three wire system will be considered.

The corresponding stator and rotor d-q current vectors are

$$\mathbf{i}^e_{qds} = \left[i^e_{qs}, i^e_{ds}, 0 \right]^t \quad (6)$$

$$\mathbf{i}^e_{qdr} = \left[i^e_{qr}, i^e_{dr}, 0 \right]^t \quad (7)$$

The angular velocity vector of the flux vector is

$$\boldsymbol{\omega}_e = \left[0, 0, \omega_e \right]^t \quad (8)$$

In addition the following symbols are defined:

- r_s: stator resistance
- r_r': rotor resistance (referred to the stator)
- L_m: stator/rotor mutual inductance
- L_s: stator self inductance
- L_r': rotor self inductance (referred to the stator)
- ω_r: equivalent two pole rotor mechanical angular velocity
- T_e: electromagnetic torque
- T_L: load torque
- P: number of poles
- J: total moment of inertia of the drive

The transformation from the physical three phase stationary variables to two phase rotating variables is readily accomplished by means of the following equations.

$$\mathbf{v}^e_{qds} = \frac{2}{3} \begin{bmatrix} \cos\omega_e t & \cos(\omega_e t - 2\pi/3) & \cos(\omega_e t + 2\pi/3) \\ \sin\omega_e t & \sin(\omega_e t - 2\pi/3) & \sin(\omega_e t + 2\pi/3) \\ 0 & 0 & 0 \end{bmatrix} \begin{bmatrix} v_{as} \\ v_{bs} \\ v_{cs} \end{bmatrix} \quad (9)$$

$$\mathbf{i}^e_{qds} = \frac{2}{3} \begin{bmatrix} \cos\omega_e t & \cos(\omega_e t - 2\pi/3) & \cos(\omega_e t + 2\pi/3) \\ \sin\omega_e t & \sin(\omega_e t - 2\pi/3) & \sin(\omega_e t + 2\pi/3) \\ 0 & 0 & 0 \end{bmatrix} \begin{bmatrix} i_{as} \\ i_{bs} \\ i_{cs} \end{bmatrix} \quad (10)$$

where v_{as}, v_{bs}, v_{cs} are the three phase stator voltages and i_{as}, i_{bs}, i_{cs} are the three stator phase currents. An equation similar to Eq. 9 applies for the transformation of rotor currents except that the angular frequency ω_e is replaced by the slip angular frequency $\omega_s = \omega_e - \omega_r$.

The Indirect Vector Control Technique

The principle employed for indirect vector control can be understood if the current variables of Eqs. 1 and 2 are replaced by equivalent flux linkages. In particular, the rotor flux vector $\boldsymbol{\lambda}^e_{qdr}$ in the synchronously rotating reference frame can be written in terms of the stator and rotor d-q current vectors as

$$\boldsymbol{\lambda}^e_{qdr} = L_m \mathbf{i}^e_{qds} + L_r' \, \mathbf{i}^e_{qdr} \quad (11)$$

The stator current vector $\mathbf{i}^e_{qds}$ can be expressed in terms of the rotor flux vector λ^e_{qdr}, the slip angular frequency ω_s and the induction motor parameters by eliminating the rotor current vector $\mathbf{i}^e_{qdr}$ from Eq. 2 using Eq. 11. The result is

$$\mathbf{i}^e_{qds} = \frac{1}{L_m} \boldsymbol{\lambda}^e_{qdr} + \frac{L_r'}{L_m r_r'} \frac{d}{dt} \boldsymbol{\lambda}^e_{qdr} + \frac{L_r'}{L_m r_r'} \boldsymbol{\omega}_s \times \boldsymbol{\lambda}^e_{qdr} \quad (12)$$

Figure 2 shows the resulting vector diagram of the stator current in the synchronously rotating reference frame for the particular case where the d-axis is aligned with the rotor flux vector. It can be noted that, in this case, the rotor flux vector $\boldsymbol{\lambda}^e_{qdr}$ has only one non zero component $-\lambda^e_{dr}$. The d and q components of the stator current vector thereby reduce to the following:

$$i^e_{qs} = \frac{L_r'}{L_m r_r'} \omega_s \, \lambda^e_{dr} \quad (13)$$

$$i^e_{ds} = \frac{1}{L_m} \lambda^e_{dr} + \frac{L_r'}{L_m r_r'} \frac{d}{dt} \lambda^e_{dr} \quad (14)$$

The electrical angle between the stator current and rotor flux vectors is

$$\alpha = \tan^{-1} \frac{i^e_{qs}}{i^e_{ds}} \quad (15)$$

The electromagnetic torque, Eq. 3, can now be expressed in terms of only the q component of the stator current vector i^e_{qs} and the d component of the rotor flux vector λ^e_{dr} as

$$T_e = \frac{3}{2} \frac{P}{2} \frac{L_m}{L_r'} \lambda^e_{dr} \, i^e_{qs} \quad (16)$$

It can be noted that Eq. 16 has the same form as the torque equation of a DC machine. Hence it is a key result since it implies that control strategies similar to that employed for DC machines can be used to control an induction

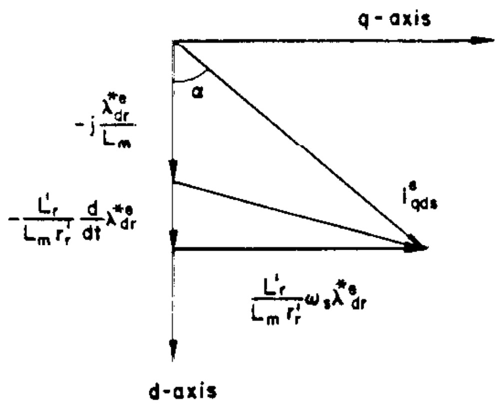

Fig. 2 Vector Diagram of Stator Current and Rotor Flux Linkage in the Synchronously Rotating Reference Frame.

motor. In particular, shunt DC motor control principles can be adapted to induction motor control wherein the electromagnetic torque and the rotor flux are controlled independently by regulating the d and q components of stator current together with slip frequency using the following relationships obtained from Eqs. 13, 14 and 16,

$$i_{qs}^{e*} = \frac{4}{3P}\frac{L_r'}{L_m}\frac{T_e^*}{\lambda_{dr}^{*e}} \tag{17}$$

$$i_{ds}^{e*} = \frac{1}{L_m}\lambda_{dr}^{*e} + \frac{L_r'}{L_m r_r'}\frac{d}{dt}\lambda_{dr}^{*e} \tag{18}$$

$$\omega_s^* = \frac{4}{3P} r_r' \frac{T_e^*}{\left[\lambda_{dr}^{*e}\right]^2} \tag{19}$$

where T_e^* and λ_{dr}^{*e} are the desired values of torque and rotor flux. In these equations the asterisk denotes the commanded value of the variable. The rotor slip frequency ω_s can only be controlled indirectly by means of the PWM inverter. The necessary stator frequency command to the inverter can be obtained by simply summing the commanded slip frequency with the measured rotor frequency (i.e. speed).

$$\omega_e^* = \omega_r + \omega_s^* \tag{20}$$

While Eqs. 17-20 are sufficient to define the input conditions to the motor, the stator current commands in the synchronously rotating reference frame $\mathbf{i}_{qds}^{e*} = [i_{qs}^{e*}, i_{ds}^{e*}, 0]^t$ must now be converted to the stationary reference frame since the stator current of the induction motor can be only controlled by a static inverter in the stationary reference frame. The stator current command in the stationary reference frame $\mathbf{i}_{qds}^{s*}$ can be obtained by the inverse transformation to Eq. 10 where the commanded values of stator current replace the actual values. That is

$$\begin{bmatrix} i_{as}^* \\ i_{bs}^* \\ i_{cs}^* \end{bmatrix} = \begin{bmatrix} \cos\omega_e^* t & \sin\omega_e^* t & 0 \\ \cos(\omega_e^* t - 2\pi/3) & \sin(\omega_e^* t - 2\pi/3) & 0 \\ \cos(\omega_e^* t + 2\pi/3) & \sin(\omega_e^* t + 2\pi/3) & 0 \end{bmatrix} \mathbf{i}_{qds}^{e*} \tag{21}$$

A block diagram configuration for field oriented control of an induction motor implementing Eqs. 17-20 is shown in Fig. 3. Note that the set points for the stator current and frequency are obtained without benefit of a flux measurement. Hence, the so- called indirect field oriented control scheme has been realized. In Fig. 3 the overall vector controller generates instantaneous three phase current commands i_{as}^*, i_{bs}^* and i_{cs}^* from the torque command T_e^* and the rotor flux command λ_{dr}^{*e} and a speed feedback signal. The d-q coordinate stator current commands in the synchronously rotating reference frame, i_{qs}^{e*} and i_{ds}^{e*}, and the slip frequency command, ω_s^*, are obtained from the torque command T_e^* and the rotor flux command λ_{dr}^{*e} according to the Eqs. 17, 18 and 19. For simplicity the transformation of current commands from the synchronous to the stationary from is done in a two stage process. First, the corresponding d-q coordinate stator current commands in the stationary reference frame, $\mathbf{i}_{qds}^{s*}$, are obtained by changing coordinates from the synchronously rotating reference frame to the stationary reference frame. The stationary d-q coordinate stator current command is then transformed to three phase current commands. A static PWM inverter is subsequently used to realize the desired three phase currents in the induction motor.

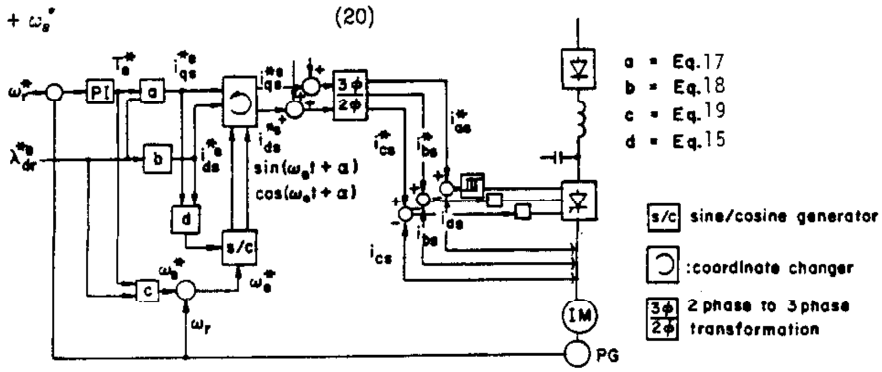

Fig. 3 System Simulated on Analog Computer Incorporating Modified Vector Controller and Current Regulated Hysteresis Type PWM Inverter.

Analog Computer Simulation of Vector Controlled Drive

Before discussion of the control component of the computer simulation, it is useful to review the equations necessary to implement the power portion of the system, i.e. the induction motor and the dc link filter.

Machine Simulation Equations

As is usually the case, it is convenient to simulate the induction machine in the stationary reference frame even though the concept of field oriented control utilizes the synchronous reference frame. The simulation equations for an induction motor in the stationary reference frame are typically expressed in the form shown below [6].

$$\psi_{qs} = \omega_b \int \left[v_{qs} + \frac{r_s}{X_{ls}} \left(\psi_{mq} - \psi_{qs} \right) \right] dt \quad (22)$$

$$\psi_{ds} = \omega_b \int \left[v_{ds} + \frac{r_s}{X_{ls}} \left(\psi_{md} - \psi_{ds} \right) \right] dt \quad (23)$$

$$\psi_{qr}' = \omega_b \int \left[\frac{\omega_r}{\omega_b} \psi_{dr}' + \frac{r_r'}{X_{lr}'} \left(\psi_{mq} - \psi_{qr}' \right) \right] dt \quad (24)$$

$$\psi_{dr}' = \omega_b \int \left[- \frac{\omega_r}{\omega_b} \psi_{qr}' + \frac{r_r'}{X_{lr}'} \left(\psi_{md} - \psi_{dr}' \right) \right] dt \quad (25)$$

$$\psi_{mq} = \frac{X_m^*}{X_{ls}} \psi_{qs} + \frac{X_m^*}{X_{lr}'} \psi_{qr}' \quad (26)$$

$$\psi_{md} = \frac{X_m^*}{X_{ls}} \psi_{ds} + \frac{X_m^*}{X_{lr}'} \psi_{dr}' \quad (27)$$

$$i_{qs} = \frac{\left(\psi_{qs} - \psi_{mq} \right)}{X_{ls}} \quad (28)$$

$$i_{ds} = \frac{\left(\psi_{ds} - \psi_{md} \right)}{X_{ls}} \quad (29)$$

$$i_{qr}' = \frac{\left(\psi_{qr}' - \psi_{mq} \right)}{X_{lr}'} \quad (30)$$

$$i_{dr}' = \frac{\left(\psi_{dr}' - \psi_{md} \right)}{X_{lr}'} \quad (31)$$

$$T_e = \frac{3}{2} \frac{P}{2} \frac{1}{\omega_b} \left(\psi_{ds} \, i_{qs} - \psi_{qs} \, i_{ds} \right) \quad (32)$$

$$\frac{\omega_r}{\omega_b} = \frac{P}{2 J \omega_b} \int \left(T_e - T_L \right) dt \quad (33)$$

In these equations ψ denotes the so-called pitch-fork (base angular frequency) flux linkage defined as

$$\psi = \omega_b \, \lambda \quad (34)$$

where λ is the flux linkage in weber turns for a particular magnetic circuit. It is interesting to note that the units for ψ are *volts* which makes the simulation of this quantity particularly convenient.

In addition, in Eqs. 22-33

$$X_m^* = \frac{1}{\frac{1}{X_{ls}} + \frac{1}{X_{lr}'} + \frac{1}{X_m}} \quad (35)$$

and

ω_b : base angular frequency

X_{ls} : stator leakage impedance at base frequency

X_{lr}' : rotor leakage impedance at base frequency (referred to the stator)

X_m : magnetizing impedance at base frequency

r_r' : rotor resistance (referred to the stator)

r_s : stator resistance

The values of the motor parameters used in the simulation are listed in Appendix A.1.

The completed d,q domain analog computer simulation diagram in the stationary reference frame for the induction motor is illustrated in Fig. 4. The definitions of the analog computer symbols used in the simulation diagram are listed in the Appendix A.2.

Filter Simulation Equations

The circuit and simulation diagram for a single stage dc link filter are shown in Fig. 5. For simplicity, an ideal adjustable amplitude voltage source has been assumed for the rectifier. If desired, a detailed simulation of the rectifier can be carried out by previously published techniques [7]. The simulation diagram for the dc filter is obtained by the following simulation equations.

$$V_I = \frac{1}{C} \int I_C \, dt \quad (36)$$

$$I_C = I_L - I_I \quad (37)$$

$$I_L = \frac{1}{L} \int \left(V_R - V_I - R \, I_L \right) dt \quad (38)$$

A diode connected around the integrator used to develop the inductor (rectifier) current I_L can be noted. This diode is used to ensure that undirectional current only can flow from the input rectifier. Figure 5 also shows the presence of three switches which act in unison to form the inverter dc link current. The corresponding computer mechanization of the inverter voltages and the dc link inverter voltage is given in Fig. 6. The switches of Figs. 5 and 6 act in unison in response to switching command generated in the control portion of the inverter simulation. Figure 6 also shows the implementation of the transformation equations from three phase to two phase which are expressed as follows.

$$v_{qs} = \frac{1}{3} \left(2 \, v_{as} - v_{bs} \; v_{cs} \right) \quad (39)$$

$$v_{ds} = \frac{1}{\sqrt{3}} \left(v_{cs} - v_{bs} \right) \quad (40)$$

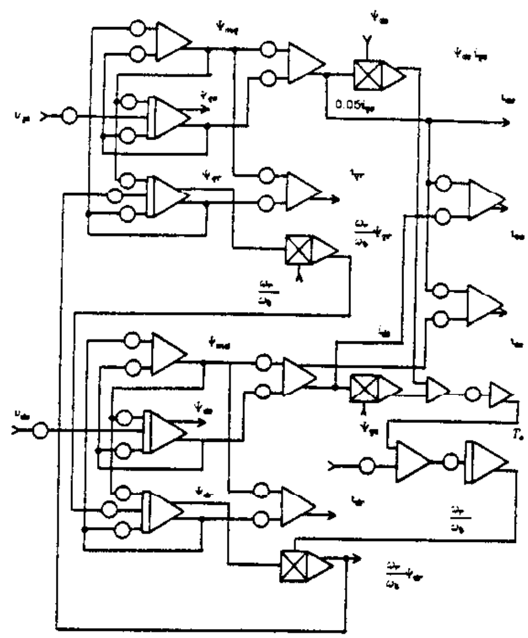

Fig. 4 A d,q Axes Simulation Diagram for an Induction Motor in the Stationary Reference Frame.

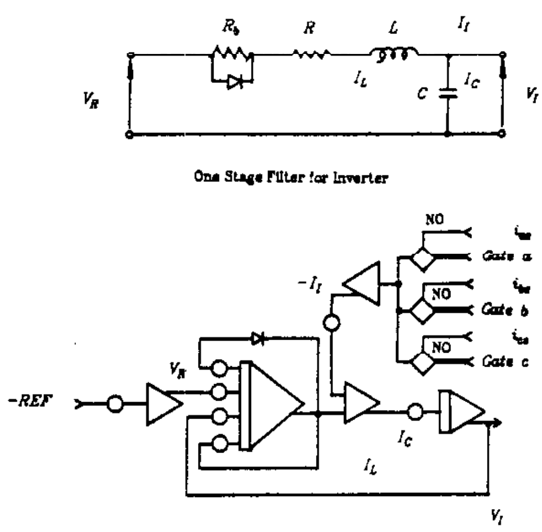

Fig. 5 (a) Equivalent Circuit of Single Stage Filter, (b) Analog Computer Simulation.

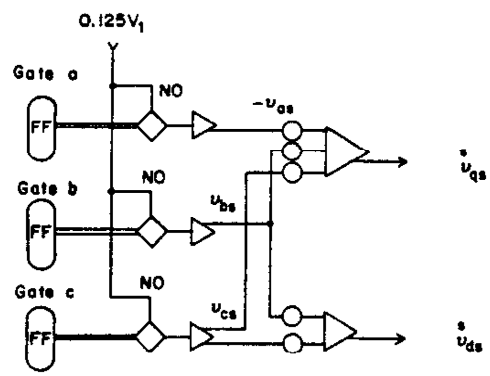

Fig. 6 Simulation Diagram for Mechanization of Inverter Voltages.

Control Simulation

The gate pulse generator of a hysteresis type current controlled voltage source inverter is shown in Fig. 7. In hysteresis type regulation, the three phase currents of the induction motor are controlled to follow the current commands by switching the output voltages of the inverter. The current is specified to be maintained between $i^* + \Delta i^*_{bias}$ and $i^* - \Delta i^*_{bias}$. The relationships between the inverter gate pulses and the current is as follows:

If: $i_{as} < i^*_{as} - \Delta i^*_{bias}$

Then: Gate **a** is true

If: $i^*_{as} - \Delta i^*_{bias} < i_{as} < i^*_{as} + \Delta i^*_{bias}$

Then: Gate **a** is previous state

If: $i^*_{as} + \Delta i^*_{bias} < i_{as}$

Then: Gate **a** is false.

Figures 8, 9 and 10 show the simulation diagrams for the field oriented controller. It can be noted that the motor torque and the rotor flux are controlled separately and the controller generates the appropriate three phase current commands in the stationary reference frame whereby the decoupling of these two functions can be accomplished. The desired rotor flux is assumed to be constant in this model but can adjustments be easily accomodated by proper adjustment of the current command i^*_{qs}.

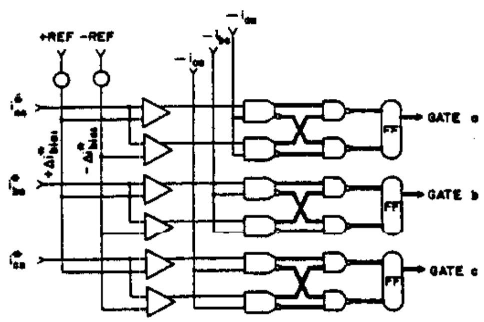

Fig. 7 Analog Computer Simulation of Hysteresis Type Gate Pulse Generator for PWM Inverter.

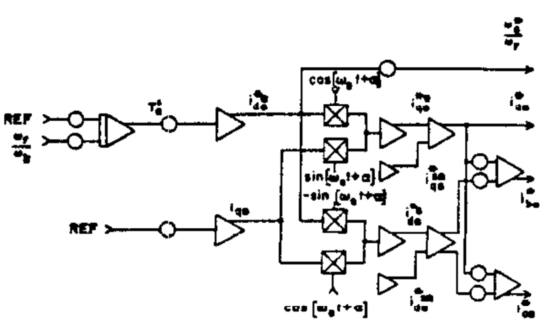

Fig. 8 Simulation Diagram for Field Oriented Controller Showing Independent Regulation of Flux and Torque and Transformation from Rotating to Stationary Axes.

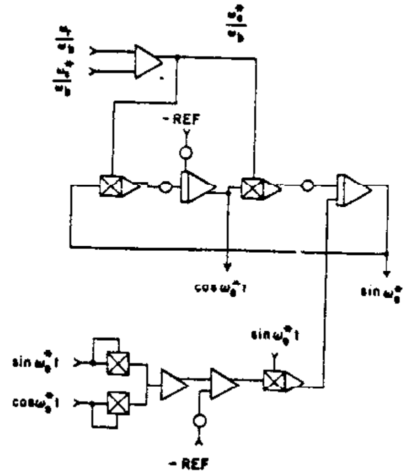

Fig. 9 Simulation Diagram Showing Mechanization of Variable Frequency Generator for Reference Frame Transformation.

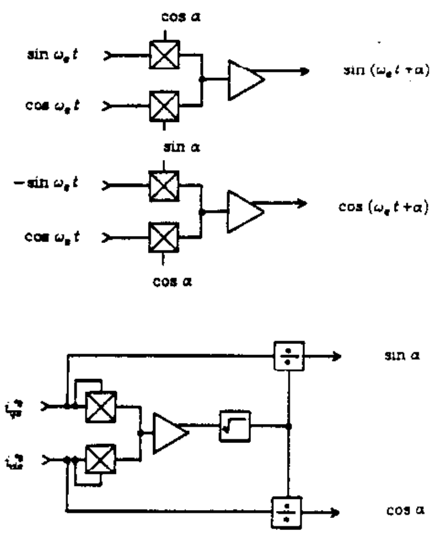

Fig. 10 Simulation Diagram Showing Phase Shifter for Decoupling of Torque and Flux Commands.

Simulation Results

Figure 11 shows the analog traces of the waveforms of the current command i^*_{as}, the motor phase current i_{as} and the gate pulses of the inverter. Figure 12 shows the analog traces of the inverter gate pulses, three phase voltages, v_{as}, v_{bs} and v_{cs}, and d-q voltages, v_{qs} and v_{ds}. Figure 13 shows the analog traces of the three phase current commands, i^*_{as}, i^*_{bs} and i^*_{cs}, the inverter currents i_{as}, i_{bs} and i_{cs} and the d-q currents, i_{qs} and i_{ds}. All three traces were taken with the example 175 HP motor operating at rated load and frequency (see Appendix 1). It is apparent that the hysteresis type of current control scheme is an excellent one. However, it should be noted that a proper turn off time margin must be required because of the limitation of the turn off capability of the power devices in the actual system.

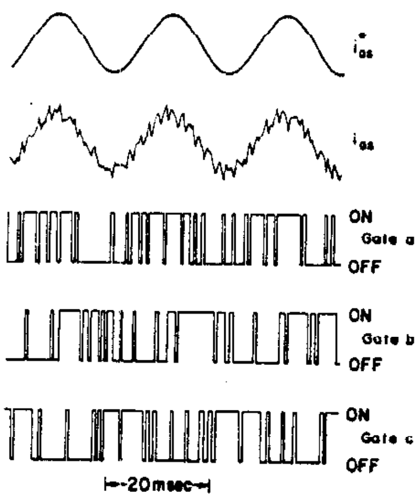

Fig. 11 Computer Traces Showing Current Command Signal, Resulting Motor Current and Inverter Gate Pulses.

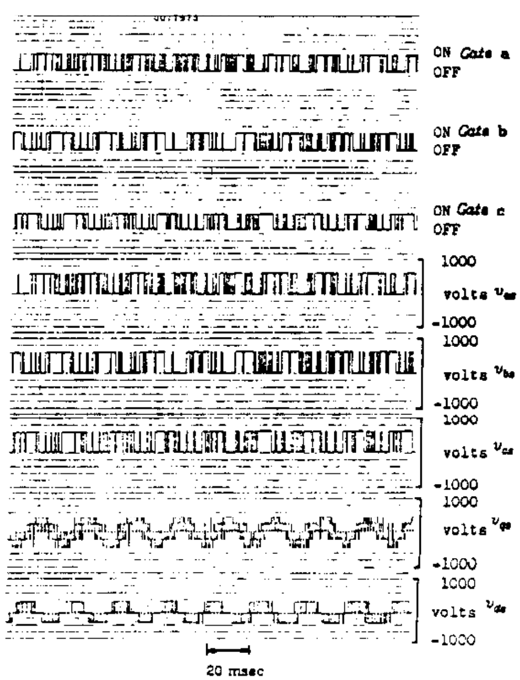

Fig. 12 Simulation Traces of Inverter Gate Pulses and Inverter Voltages.

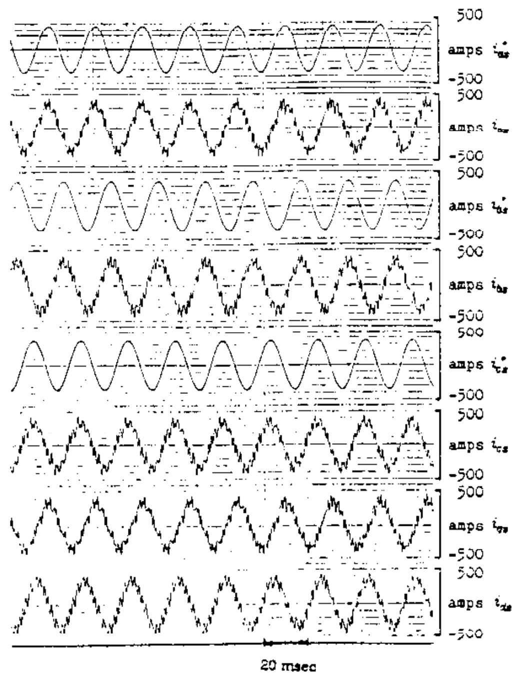

Fig. 13 Chart Recorder Traces of Current Commands and Resulting Inverter Currents.

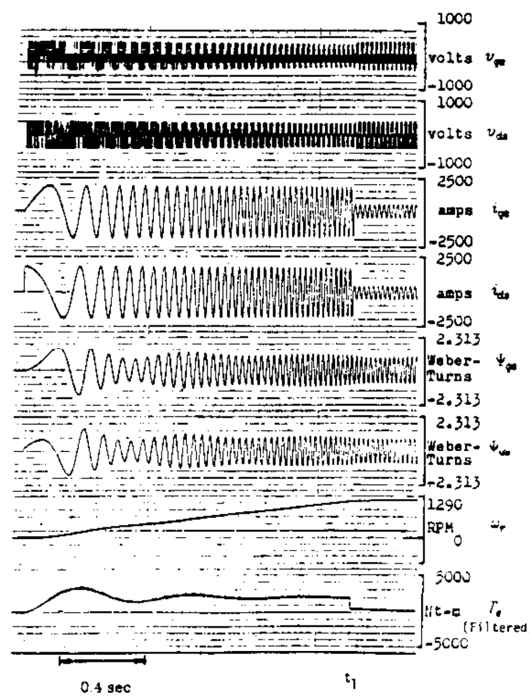

Fig. 14 Computer Traces of Acceration of Induction Motor from Rest Using an Indirect Field Oriented Control. Note the Step Change in Load Torque at $t=t_1$.

Figure 14 shows the analog traces of an induction motor driven by the current control type voltage source inverter with slip frequency control type field oriented controller, where the induction motor is accelerated from zero speed to full speed under the constant torque command. When the motor arrives at its commanded speed, the load torque has been suddenly changed. A nearly instantaneous response, characteristic of field oriented type control systems is evident.

Conclusion

Induction motor control by field orientation is presently considered as one of the prime candidates to take the place of dc motor drives. In particular, the *slip frequency* or *indirect* type of field oriented control system is considered to be the most practical systems because 1) it does not require a flux sensor. Hence, it can be applied to induction motor drives systems which are already in operation. 2) The approach is readily adapted to the use of microprocessors. The design and development of such a system is a costly and difficult procedure. This paper has presented the details of an analog computer implementation of such a controller which can be conveniently used to assist the designer with hardware implementation. While an analog computer has been found to be the most desirable tool due to its high computational speed, the block diagrams discussed in this paper are equally amenable to a digital computer simulation using software such as ACSL, SuperSceptre or Easy 5.

Acknowledgments

The financial support of Mr. T. Matsuo by Mitsubishi Electric Company while at the University of Wisconsin is gratefully acknowledged. Also, the authors wish to thank the sponsors of the Wisconsin Electric Machines and Power Electronics Consortium (WEMPEC) for facilities and funds provided.

References

[1] K. Hasse, "Zur Dynamik Drehzahlgeregelter Antriebe mit Stomrichtergespeisten Asynchron-Kurzschlusslaufer-machinen", (On the Dynamics of Speed Control of Static AC Drives with Squirrel- Cage Induction Machines), Ph.D. Dissertation , TH Darmstadt, 1969.

[2] L. J. Garces, "Parameter Adaptation for the Speed-Controlled Static AC Drive with a Squirrel-Cage Induction Motor", IEEE / IAS Transactions Vol.IA-16, No.2, 1980, pp. 173-178.

[3] R. Gabriel and W. Leonhard, "Microprocessor Control of Induction Motor", IEEE/IAS International Semiconductor Power Converter Conference, May 24-27, 1982, pp. 385-396.

[4] T. Okuyama, et. al., "High Performance AC Motor Speed Control System Using GTO Converters", IPEC-TOKYO Conf. Rec., March 27-31, 1983, pp. 720-731.

[5] T.A. Lipo, "A Cartesian Vector Approach to Reference Frame Theory of AC Machines", International Conference on Electrical Machines, Lausanne, Switzerland, Sept. 18-21, 1984, (to appear).

[6] P.C. Krause and C.H. Thomas, "Simulation of Symmetrical Induction Machinery", IEEE Trans. on Power Apparatus and Systems, vol. PAS- 84, Nov. 1965, pp. 1038-1-53.

[7] H. Winograd, L. Nickels, and R. Hedin, "Design of HVDC Power Supply for Experimental DC Transmission Test Facility", Paper CP63-344, IEEE Winter Meeting, New York, 1963.

Appendix A.1
Induction Motor Parameters

Table A.1 shows the parameters of the induction motor used for the analog computer simulation. The rated horsepower of the machine is 175 HP at 1290 RPM. The resistances and reactances are the conventional per phase equivalent circuit parameters referred to the stator.

Table A.1

Induction Motor Parameters

Quantity	Symbol	Value
Phase Voltage	V_b	270 V RMS
Base Frequency	ω_b	270.2 *rad/sec*
Stator Resistance	r_s	0.0217 Ω
Stator Referred Rotor Resistance	r_r'	0.0329 Ω
Stator Leakage Reactance	X_{ls}	0.0874 Ω
Stator Referred Rotor Leakage Reactance	X_{lr}'	0.0996 Ω
Magnetizing Reactance	X_m	3.6493 Ω
Total Rotational Inertia	J	11.4 $Kg-m^2$
Number of Poles	P	4

Appendix A.2
Simulation Symbols and Their Meaning